

Interstellar Scintillation Velocities of a Relativistic Binary PSR B1534+12 and Three Other Millisecond Pulsars

Slavko Bogdanov

*Department of Astronomy and Astrophysics, Penn State University
University Park, PA 16802, USA
bogdanov@astro.psu.edu*

Małgorzata Pruszyńska and Wojciech Lewandowski

*Toruń Centre for Astronomy, Nicolaus Copernicus University
ul. Gagarina 11, 87-100 Toruń, Poland
mare@astro.uni.torun.pl, boe@astro.uni.torun.pl*

Alex Wolszczan

*Department of Astronomy and Astrophysics, Penn State University
University Park, PA 16802, USA
Toruń Centre for Astronomy, Nicolaus Copernicus University
ul. Gagarina 11, 87-100 Toruń, Poland
alex@astro.psu.edu*

ABSTRACT

We present interstellar scintillation velocity measurements for four millisecond pulsars obtained from long-term monitoring observations with the Arecibo radio telescope at 430 MHz. We also derive explicit expressions that relate the measured scintillation velocity to the effective transverse velocity responsible for the motion of the diffraction pattern for both binary and solitary pulsars. For B1257+12, B1534+12, J1640+2224, and J1713+0747 we derive ISS velocity estimates of 197 ± 57 , 192 ± 63 , 38 ± 8 , and 82 ± 16 km s⁻¹, respectively. These values are in good agreement with proper motion measurements for the four pulsars. For a relativistic binary pulsar PSR B1534+12, we use the ISS velocity dependence on orbital phase to determine the longitude of the ascending node Ω of the pulsar's orbit and to derive an estimate of the effective scattering screen location. The two possible values of Ω are 70 ± 20 and 290 ± 20 degrees and the approximate screen location is 630 ± 200 pc with the assumed pulsar distance of 1.1 kpc.

Subject headings: pulsars — interstellar medium — pulsars: relativistic binaries — pulsars: individual (PSR B1257+12, PSR B1534+12, PSR J1640+2224, PSR J1713+0747)

1. INTRODUCTION

Interstellar scintillation (ISS) of pulsars is caused by diffraction and refraction of radio waves from electron density irregularities in the interstellar plasma (Rickett 1990). Measurements of the ISS related modifications of the pulsar signal, such as the angular source broadening, temporal broadening of pulses and their intensity variations in time and frequency, have been used to study the small-scale structure of the interstellar plasma (e.g. Cordes, Weisberg, & Boriakoff 1985; Lambert & Rickett 2000).

Pulsars are fast moving objects with mean velocities of $\sim 460 \text{ km s}^{-1}$ (Lyne & Lorimer 1994) and $\sim 85 \text{ km s}^{-1}$ (Toscano et al. 1999) for the normal and the millisecond pulsar populations, respectively. Therefore, measurements of a net speed of the interstellar diffraction pattern derived from decorrelation scales of pulse intensity variations in time and frequency are dominated by the pulsar motion and can be used to estimate a transverse component of the pulsar velocity in space. In fact, the ISS technique has been routinely used as one of the means to measure pulsar velocities (e.g. Lyne & Smith 1982; Cordes 1986; Gupta, Rickett, & Lyne 1994), in addition to the more direct methods of pulse timing (e.g. Toscano et al. 1999) and radio interferometry (e.g. Fomalont et al. 1997). As the latter two techniques are limited to low timing noise, bright, nearby objects, the ISS observations provide a very helpful, additional way to obtain velocity estimates for a relatively large number of sources. Such measurements, in combination with simulation studies (Tauris & Bailes 1996; Cordes & Chernoff 1997) are important for global characterization of the galactic population of neutron stars.

The ISS velocity measurements, when combined with timing or interferometric astrometry data, provide useful constraints on the distribution of scattering material along the pulsar line of sight and provide a way to verify a reliability of the ISS method itself (Cordes & Rickett 1998; Deshpande & Ramachandran 1998). Recent analyses of a growing body of such measurements have shown that, despite their obvious model dependence, the ISS velocities are remarkably accurate (Gupta 1995; Johnston, Nicastro, & Koribalski 1998; Nicastro et al. 2001).

In principle, the ISS observations of binary pulsars can be used to track their orbital

velocities projected onto the plane of the sky and to deduce some orbital parameters that would be impossible to measure in any other way (Lyne 1984; Dewey, Cordes, & Wolszczan 1988). This is particularly true for relativistic binaries, in which case the orbital velocity variations are exceptionally large and may dominate the ISS measurements.

In this paper, we present ISS velocity measurements of four millisecond pulsars obtained from long-term monitoring observations with the 305-m Arecibo radio telescope. PSR J1640+2224 (Foster et al. 1995) and PSR J1713+0747 (Foster, Wolszczan, & Camilo 1993) are binary millisecond pulsars in long period, nearly circular orbits with white dwarf companions. PSR B1257+12 is a fast moving solitary millisecond pulsar with a system of at least three planets around it (Wolszczan & Frail 1992; Wolszczan 1994). Finally, PSR B1534+12 is a relativistic 10-hour binary pulsar in orbit with another neutron star (Wolszczan 1991; Stairs et al. 1998). Here, we focus our attention on PSR B1534+12 and the measurements of changes in its ISS velocity caused by orbital motion. We also verify the earlier ISS speed measurements for PSR B1257+12 and PSR J1713+0747 (Johnston et al. 1998; Gothoskar & Gupta 2000) and provide the first such measurement for PSR J1640+2224.

2. OBSERVATIONS AND ANALYSIS OF THE DYNAMIC SPECTRA

The four pulsars discussed in this paper have been regularly monitored with the Arecibo radio telescope to measure their pulse arrival times. The most recent results of timing modeling of these objects will be presented elsewhere. We have reprocessed the timing measurements made at multiple epochs between 1994 and 2001 at 430 MHz to obtain the dynamic spectra of pulsar scintillations and analyzed them to estimate the ISS velocities of the pulsars themselves.

Typically, PSR B1257+12, PSR J1640+2224 and PSR J1713+0747 were observed for 45-120 min. in a series of 3 min. integrations carried out synchronously with the Doppler-corrected pulsar period. In the case of PSR B1534+12, the dynamic spectra were analyzed in 45-60 min. sections to avoid excessive averaging over changes in the frequency and time decorrelation scales induced by the pulsar's orbital motion. Similarly, to eliminate biases in the decorrelation scales introduced by refractive scintillation (Bhat, Rao, & Gupta 1999) the dynamic spectra strongly affected by drifts of spectral features and quasiperiodic fringing were excluded from the analysis.

The left- and right-hand circularly polarized pulsar signals were fed into the Penn State Pulsar Machine (PSPM), which is a $2 \times 128 \times 60$ kHz channel, computer controlled, on-line pulsar processor. After detection, the dual-channel signals were added together, smoothed, 4-

bit quantized and pulse phase averaged by the analysis computer in each of the 128 frequency channels. In the off-line processing, the 128×60 kHz point spectra of the pulsar signal were formed from the ON-pulse and OFF-pulse level measurements in each frequency channel by calculating the corresponding (ON-OFF)/OFF spectral intensities. A dynamic spectrum of the pulsar intensity variations in time and frequency was then constructed from a set of 3-minute averaged, contiguous spectra for each object and each observing session.

Examples of the dynamic spectra of the four pulsars are shown in Figures 1 and 2. Also shown are the two-dimensional autocorrelation functions of these spectra, which were used to measure the decorrelation scales of pulsar intensity variations, Δt_d and $\Delta \nu_d$. Following the established convention, Δt_d and $\Delta \nu_d$ were measured as the respective $1/e$ widths and half-widths of elliptical Gaussians least-squares fitted to the autocorrelation functions. The decorrelation widths for PSR B1257+12, PSR B1534+12, PSR J1640+2224 and PSR J1713+0747, averaged over all observing epochs are listed in Table 1.

The errors of Δt_d and $\Delta \nu_d$ measurements consist of statistical uncertainty due to a finite number of “scintles” in the dynamic spectra, the signal strength, and the long-term changes of these parameters caused by refractive effects (Bhat et al. 1999). We found that the refraction induced variations in Δt_d and $\Delta \nu_d$ occurring on the time scales from months to years were a dominant source of error for all the four pulsars discussed here. Consequently, the errors quoted in Table 1 were calculated from the scatter in the estimates of the decorrelation widths over the entire time span of observations.

3. THE ISS VELOCITY ANALYSIS

The ISS velocities of pulsars can be calculated from their dynamic spectra, because the two observables, the characteristic decorrelation scales of pulse intensity in time, Δt_d , and in frequency, $\Delta \nu_d$ are directly related to the net speed of a diffractive scintillation pattern (Lyne & Smith 1982). For Δt_d and $\Delta \nu_d$ measured in seconds and megahertz, respectively, the velocity V_{ISS} (km s^{-1}) is derived from the equation (Gupta et al. 1994):

$$V_{ISS} = 3.85 \times 10^4 \frac{\sqrt{\Delta \nu_d d x}}{\nu \Delta t_d}, \quad (1)$$

where x is the ratio of the distances of the scattering screen to the observer and to the pulsar, d is the pulsar distance (in kpc), and ν is the observing frequency (in GHz). The numerical constant is valid for the assumed homogeneous turbulent medium characterized by a Kolmogorov turbulence spectrum.

In principle, the observed ISS velocity of a pulsar represents the net effect of the pulsar’s

motion, the Earth’s orbital motion around the Sun, and the motion of the scattering medium. Thus, V_{ISS} can be written as the magnitude of the vector sum of all the velocities contributing to it (Gupta et al. 1994):

$$V_{ISS} = |x\mathbf{V}_o + x\mathbf{V}_{pm} + \mathbf{V}_\oplus - (1+x)\mathbf{V}_{ism}|_\perp \quad (2)$$

where, for binary pulsars, \mathbf{V}_o is the pulsar’s orbital velocity, \mathbf{V}_{pm} is its proper motion velocity, \mathbf{V}_\oplus is the velocity of the Earth, and \mathbf{V}_{ism} is the velocity of the scattering screen. The subscript \perp indicates that the only contributions to the ISS velocity come from the components of the velocity vectors perpendicular to the line of sight. Choosing the origin of a coordinate system to coincide with the center of mass of a binary with its x-y plane tangent to the sky, with the x-axis parallel to the orbit’s line of nodes and the z-axis pointing from the solar system barycenter to that of the binary system, V_{ISS} can be expressed in terms of the projections of the component velocity vectors onto the plane of the sky:

$$V_{ISS}^2 = (xV_{o,x} + xV_{pm,x} + V_{\oplus,x})^2 + (xV_{o,y} + xV_{pm,y} + V_{\oplus,y})^2 \quad (3)$$

In this expression we have assumed that the contribution of V_{ism} to V_{ISS} is negligible (Gupta 1995). The component velocities in Eqn. (3) are defined as follows. The orbital velocity components are:

$$V_{o,x} = \xi \left\{ [e \sin \phi \cos \phi - (1 + e \cos \phi) \sin \phi] \cos \omega - [e \sin \phi \sin \phi + (1 + e \cos \phi) \cos \phi] \sin \omega \right\} \quad (4)$$

$$V_{o,y} = \xi \left\{ [e \sin \phi \cos \phi - (1 + e \cos \phi) \sin \phi] \sin \omega + [e \sin \phi \sin \phi + (1 + e \cos \phi) \cos \phi] \cos \omega \right\} (\pm \cos i) \quad (5)$$

where $\xi = (2\pi a \sin i)/(P_b \sqrt{1 - e^2} \sin i)$, a is the semi-major axis, e is the eccentricity, P_b is the orbital period, ϕ is the orbital phase, ω is the longitude of periastron, and i is the orbital inclination. The two possible signs of the $\cos i$ term arise from the fact that we have no way of determining which of the two nodes of the orbit is the ascending node so both cases need to be considered. The proper motion components are defined by the familiar relationships:

$$V_{pm,x} = 4.74d(\mu_\alpha \sin \Omega + \mu_\delta \cos \Omega) \quad (6)$$

$$V_{pm,y} = 4.74d(-\mu_\alpha \cos \Omega + \mu_\delta \sin \Omega) \quad (7)$$

where Ω is the longitude of the ascending node of the orbit, defined as the position angle (reckoned from north through east) of the line of nodes measured in the plane tangent to

the sky, μ_α and μ_β are the proper motions in right ascension and declination, respectively, in units of mas yr^{-1} , and the distance d is given in kpc. Finally, the Earth velocity components are given by:

$$V_{\oplus,x} = 1.73 \times 10^{-6} [\dot{X}(-\cos \Omega \sin \delta \cos \alpha - \sin \Omega \sin \alpha) + \dot{Y}(-\cos \Omega \sin \delta \sin \alpha + \sin \Omega \cos \alpha) + \dot{Z}(\cos \Omega \cos \delta)] \quad (8)$$

$$V_{\oplus,y} = 1.73 \times 10^{-6} [\dot{X}(-\sin \Omega \sin \delta \cos \alpha + \cos \Omega \sin \alpha) + \dot{Y}(-\sin \Omega \sin \delta \sin \alpha - \cos \Omega \cos \alpha) + \dot{Z}(\sin \Omega \cos \delta)] \quad (9)$$

where α and δ are the pulsar coordinates and the parameters \dot{X} , \dot{Y} , and \dot{Z} are the components of Earth's velocity in the Solar System Barycenter coordinate system expressed in units of AU d^{-1} .

Expression (3) conveniently reduces to one for a solitary pulsar by simply neglecting the orbital motion terms and setting Ω equal to zero:

$$V_{ISS}^2 = \{x(4.74d\mu_\delta) + 1.73 \times 10^{-6}[\dot{X}(-\sin \delta \cos \alpha) + \dot{Y}(-\sin \delta \sin \alpha) + \dot{Z} \cos \delta]\}^2 + \{x(-4.74d\mu_\alpha) + 1.73 \times 10^{-6}[\dot{X} \sin \alpha - \dot{Y} \cos \alpha]\}^2 \quad (10)$$

In what follows, Eq. (1) is used to derive the observed ISS velocities from ISS measurements, whereas Eq. (3) or Eq. (10) give the expected ISS speeds from the known pulsar proper motion and Earth velocities.

4. ISS VELOCITY AND ORBITAL MOTION OF PSR B1534+12

Johnston et al. (1998), Gothoskar & Gupta (2000), and Lommen (2001) have measured the ISS velocity for this pulsar to be 190 km s^{-1} , 191 km s^{-1} , and 149 km s^{-1} , respectively. In principle, these estimates can be significantly biased by a varying transverse component of the pulsar's orbital velocity, whose semi-amplitude exceeds $\sim 100 \text{ km s}^{-1}$. Here we have performed a rigorous analysis of this effect by taking into account all the motions contributing significantly to the observed ISS velocity of PSR B1534+12, as well as the dependence of the ISS velocity on the pulsar's orbital phase.

Compared to the results of similar analyses carried out for the binary pulsars PSR B0655+64 by Lyne (1984) and PSR B1855+09 and PSR B1913+16 by Dewey et al. (1988),

the ISS velocities for PSR B1534+12 shown in Fig. 3 exhibit a much more pronounced dependence on orbital phase and allow an unambiguous modeling of this effect with the aid of Eqs. (3-9). In fact, the problem can be conveniently parametrized in terms of only two unknowns, the longitude of the ascending node Ω and the screen location x , with the Keplerian orbital parameters and proper motion of the pulsar already determined from long-term timing measurements (Stairs et al. 1998, and references therein). For the pulsar distance we have adopted a value of $d = 1.1 \pm 0.2$ kpc derived by Stairs et al. (1998) on the assumption that General Relativity (GR) is the correct theory of gravity.

Although the longitude of periastron ω of the pulsar’s orbit advances at a rate of 1.75 deg yr^{-1} , it does not change fast enough to have a significant effect on our analysis. Consequently, we have used the value of ω at the mid-point of the actual observing period. Finally, because the transverse component of the Earth’s velocity varies and its direction relative to the pulsar’s orbital motion cannot be determined without knowing Ω , we have ignored the V_{\oplus} terms in Eq. (3) and included them in the uncertainties of the V_{ISS} measurements.

Since both the model (Eq. 3) and Eq. (1) include a dependence on the parameter x , the best fit values of Ω and x were obtained by manually searching the χ^2 -space for the minimum. The fit yielded $\Omega_1 = 70 \pm 20$ and $\Omega_2 = 290 \pm 20$ degrees for the longitude of the ascending node and $x = 1.3 \pm 0.4$, which corresponds to a screen located at a distance of $d_s = 630 \pm 200$ pc from the Earth. Fig. 3 shows the ISS velocity measurements of PSR B1534+12 and the best fitting curve given by Eq. (3) plotted against orbital phase.

From our ISS velocity measurements of PSR B1534+12 it is also possible to give an estimate of the pulsar’s transverse systemic velocity. Since the transverse component of the pulsar’s orbital velocity never vanishes the best we can do is to consider only the measurements made around orbital phases 0.2 and 0.7 at which it reaches the minimum value. Using these measurements we obtain a value of 192 km s^{-1} , which is an overestimate of the actual proper motion due to contributions from the pulsar’s orbital motion as well as the location of a scattering screen. Nonetheless, this value is remarkably close to those published by Johnston et al. (1998) and Gothoskar & Gupta (2000).

5. ISS VELOCITIES OF PSR B1257+12, PSR J1640+2224, AND PSR J1713+0747

Scintillation velocities of PSR B1257+12 were calculated using the distance based on the Taylor & Cordes (1993) model of galactic electron distribution (the TC model hereafter). For the pulsar distance of 0.62 kpc, we obtained an average value of $V_{ISS} = 197 \pm 57 \text{ km}$

s^{-1} . The ISS velocity estimate of 225 km s^{-1} using the same distance has been derived by Gothoskar & Gupta (2000). We find these two estimates to be remarkably similar given the large, long-term variations of the ISS velocity observed for this pulsar. The measured velocity variations ranging from 117 km s^{-1} to 290 km s^{-1} on a time scale of ~ 2 years are consistent with modifications of the scintillation decorrelation scales by the refractive scintillation. We have found the ISS velocity of this pulsar to be consistently lower than the effective transverse velocity of $\sim 278 \text{ km s}^{-1}$, computed using the proper motion values given by Wolszczan et al. (2000), with the average ratio $V_{ISS}/V_{eff} = 0.67$. This difference can be plausibly accounted for by assuming that the scattering screen is located closer to the observer than to the pulsar ($x < 1$). It is also likely that the distance used is an underestimate of the true distance to the pulsar.

Our measurement of V_{ISS} of $38 \pm 8 \text{ km s}^{-1}$ for PSR J1640+2224 represents the first ISS velocity estimate for this binary millisecond pulsar. In the calculations we adopted the TC model distance of 1.18 kpc. In comparing this velocity with the value of 75 km s^{-1} obtained from Eq. (10), computed with proper motion measurements provided by Wolszczan et al. (2000), we have ignored the transverse component of the pulsar’s orbital velocity, because it is unlikely to be greater than 10 km s^{-1} . On the other hand, the transverse component of the Earth’s orbital velocity accounts for as much as 40% of the effective ISS velocity of the pulsar and it must be included in the analysis. Since the ISS velocity for PSR J1640+2224 is lower than the effective transverse velocity with the ratio $V_{ISS}/V_{eff} = 0.52$, it is likely that the effective location of the scattering screen is closer to the observer than to the pulsar. However, this discrepancy may also mean that the distance of 1.18 kpc we used may be an underestimate of the actual pulsar distance.

ISS velocity estimates of 29 km s^{-1} and $118 \pm 40 \text{ km s}^{-1}$ for PSR J1713+0747 have already been published by Johnston et al. (1998), using a distance of 0.89 kpc, and by Lommen (2001), respectively. Even if corrected for the TC distance of 1.1 kpc used here, the value given by Johnston et al. is still significantly lower than our velocity estimate of $82 \pm 16 \text{ km s}^{-1}$ and that of Lommen (2001). In absence of observations made at sufficiently similar epochs, the source of large discrepancies between the three values remains uncertain, although the refraction induced V_{ISS} variability provides a possible explanation. Since the transverse component of the orbital velocity of PSR J1713+0747 does not contribute more than $\sim 15 \text{ km s}^{-1}$ to the pulsar’s ISS velocity, we included it in the effective uncertainty of the measurement and used Eq. (10) instead of Eq. (3). With a net effective velocity of 52 km s^{-1} for this pulsar, calculated using the proper motion values given by Camilo, Foster, & Wolszczan (1994), our measurements of the ISS velocity are consistently larger than the effective transverse velocity. In this case, the ratio $V_{ISS}/V_{eff} = 1.71$ suggests either the presence of an asymmetrically located scattering screen which is closer to the pulsar than to

the observer (i.e. $x > 1$) or that the pulsar distance is overestimated.

6. DISCUSSION

We have presented measurements of interstellar scintillation velocities for four pulsars together with a complete set of relationships that should be used to compare these velocities with the proper motion measurements. Our V_{ISS} estimates are generally consistent with the corresponding proper motion based values derived from timing measurements of these objects. As shown by the results of similar analyses conducted in the past (e.g Johnston et al. 1998; Gothoskar & Gupta 2000), the discrepancies between these two kinds of the transverse pulsar velocity measurements can be accounted for by either an asymmetric location of the effective scatterer along the line of sight, or by an inaccurate estimate of the pulsar distance. In principle, these two factors can be decoupled by the analysis that involves the angular and temporal broadening data, in addition to the scintillation and proper motion measurements of a pulsar (Cordes & Rickett 1998; Deshpande & Ramachandran 1998). It is likely, that these “hybrid” methods will offer an important means to study a line-of-sight distribution of the scattering material, as timing and astrometric proper motion measurements for many more pulsars become available.

Our analysis of the relativistic binary pulsar PSR B1534+12 provides the best demonstration so far that the changes of a transverse component of the pulsar orbital velocity can be unambiguously detected in the ISS velocity data. The most important practical consequence of this detection is the measurement of the longitude of the ascending node Ω of the binary orbit. This parameter cannot be determined from pulsar timing, except in very special circumstances (Kopeikin 1996; van Straten et al. 2001). One of the instances where the knowledge of Ω is important is the effect of aberration caused by the relativistic orbital motion of a pulsar (Damour & Taylor 1992). In this case, Ω has to be taken into account in the determination of aberration-induced variations of the orbital phase dependent offset of the linear polarization angle of the pulse profile (Damour & Taylor 1992, Eqs. 2.16-2.24). The value of Ω is also needed for a precise measurement of a proper motion related rate of change of the projected size of the pulsar orbit (Kopeikin 1996, and references therein):

$$\delta\dot{x} = 1.54 \times 10^{-16} x \cot i (-\mu_\alpha \sin \Omega + \mu_\delta \cos \Omega) \quad (11)$$

where, x is the size of the projected semi-major axis expressed in seconds. From this equation we obtain values of $\delta\dot{x}_1 = -9.43 \times 10^{-16} \text{ s s}^{-1}$ and $\delta\dot{x}_2 = -1.25 \times 10^{-15} \text{ s s}^{-1}$, corresponding to Ω_1 and Ω_2 , respectively. With the currently available timing data for PSR B1534+12, this effect is not yet measurable.

Aside from the ambiguity in Ω resulting from the unknown direction of the pulsar's orbital motion, the two values of this parameter obtained from our analysis are very robust in the sense that small changes of Ω lead to the correspondingly large changes of the shape of the V_{ISS} curve (Fig. 3). On the other hand, the screen location is less well determined, because of the uncertain estimate of the pulsar distance. However, if the GR derived distance to PSR B1534+12 is reliable, it is probably safe to assume that the screen is indeed located closer to the pulsar than to the observer.

We would like to thank Ingrid Stairs for her continuing help with the PSPM observations of PSR B1534+12 and Maciej Konacki for insightful discussions. This work was supported by a National Science Foundation grant AST-9988217 (SB, AW) and a Polish Committee for Scientific Research grant 2-P03D-006-16 (WL, MP, AW). The Arecibo Observatory is part of the National Astronomy and Ionosphere Center, which is operated by Cornell University under a cooperative agreement with the NSF.

REFERENCES

- Bhat, N. D. R., Rao, A. P., & Gupta, Y. 1999, *ApJS*, 121, 483
- Camilo, F., Foster, R. S., & Wolszczan, A. 1994, *ApJ*, 437, L39
- Cordes, J. M. 1986, *ApJ*, 311, 183
- Cordes, J. M., Weisberg, J. M., & Boriakoff, V. 1985, *ApJ*, 288, 221
- Cordes, J. M., & Chernoff, D. F. 1997, *ApJ*, 482, 971
- Cordes, J. M. & Rickett, B. J. 1998, *ApJ*, 507, 846
- Damour, T., & Taylor, J. H. 1992, *Phys. Rev. D*, 45, 1840
- Deshpande, A. A. & Ramachandran, R. 1998, *MNRAS*, 300, 577
- Dewey, R. J., Cordes, J. M., & Wolszczan, A. 1988 in *AIP Conf. Proc.* 174, *Radio Wave Scattering in the Interstellar Medium*, ed. J. M. Cordes, B. J. Rickett, & D. C. Backer (New York: AIP), 217
- Fomalont, E. B., Goss, W. M., Manchester, R. N., & Lyne, A. G. 1997, *MNRAS*, 286, 81
- Foster, R. S., Wolszczan, A., & Camilo, F. 1993, *ApJ*, 410, L91
- Foster, R. S., Cadwell, B. J., Wolszczan, A., & Anderson, S. B. 1995, *ApJ*, 454, 826

- Gothoskar, P. & Gupta, Y. 2000, ApJ, 531, 345
- Gupta, Y., Rickett, B. J. & Lyne, A. G. 1994, MNRAS, 269, 1035
- Gupta, Y. 1995, ApJ, 451, 717
- Johnston, S., Nicastro, L., & Koribalski, B. 1998, MNRAS, 297, 108
- Kopeikin, S. M. 1996, ApJ, 467, L93
- Lambert, H. C. & Rickett, B. J. 2000, ApJ, 531, 883
- Lommen, A. N. 2001, PhD Thesis, University of California, Berkeley, CA
- Lyne, A. G. 1984, Nature, 310, 300
- Lyne, A. G., & Lorimer, D. R. 1994, Nature, 369, 127
- Lyne, A. G. & Smith, F. G. 1982 Nature, 298, 825
- Nicastro, L., Nigro, F., D’Amico, N., Lumiella, V., & Johnston, S. 2001, A&A, 368, 1055
- Rickett, B. J. 1990, ARA&A, 28, 561
- Stairs, I. H., Arzoumanian, Z., Camilo, F., Lyne, A. G., Nice, D. J., Taylor, J. H., Thorsett, S. E., & Wolszczan, A. 1998, ApJ, 505, 352
- Tauris, T. M & Bailes, M. 1996, A&A, 315, 432
- Taylor, J. H. & Cordes, J. M. 1993, ApJ, 411, 674
- Toscano, M., Sandhu, J. S., Bailes, M. Manchester, R. N., Britton, M. C., Kulkarni, S. R., Anderson, S. B., & Stappers, B. W. 1999, MNRAS, 307, 925
- van Straten, W., Bailes, M., Britton, M., Kulkarni, S. R., Anderson, S. B., Manchester, R. N., & Sarkissian, J. 2001, Nature, 412, 158
- Wolszczan, A. 1991, Nature, 350, 688
- Wolszczan, A. 1994, Science, 264, 538
- Wolszczan, A. & Frail, D. A. 1992, Nature, 355, 145
- Wolszczan, A., Doroshenko, O., Konacki, M., Kramer, M., Jessner, A., Wielebinski, R., Camilo, F., Nice, D. J., & Taylor, J. H. 2000, ApJ, 528, 907

Fig. 1.— (*Left*) Dynamic spectra of the interstellar scintillation of PSR B1257+12 and PSR B1534+12 measured with the Arecibo radiotelescope at 430 MHz. (*Right*) The corresponding two-dimensional autocorrelation functions. The top and right-hand side panels represent zero lag cross-sections of these functions in frequency and time, respectively.

Fig. 2.— (*Left*) Dynamic spectra of the interstellar scintillation of PSR J1640+2224 and PSR J1713+0747 measured with the Arecibo radiotelescope at 430 MHz. (*Right*) The corresponding two-dimensional autocorrelation functions. The top and right-hand side panels represent zero lag cross-sections of these functions in frequency and time, respectively.

Fig. 3.— The interstellar scintillation velocity of PSR B1534+12 at 430 MHz measured as a function of orbital phase. The best fit model of this relationship involving two free parameters, the longitude of the ascending node of the orbit Ω , and the ratio of distances of the scattering screen to the observer and the pulsar x , is shown as the solid line.

Table 1. Scintillation parameters and velocities of the pulsars B1257+12, B1534+12, J1640+2224, and 1713+0747.

PSR	d (kpc)	$\Delta\nu_d$ (MHz)	Δt_d (min)	Observed V_{ISS} (km s ⁻¹)	Predicted V_{ISS} (km s ⁻¹)
B1257+12	0.6	1.1 ± 0.8	6 ± 2	197 ± 57	278 ± 16
B1534+12	1.1	1.1 ± 0.4	11 ± 3	192 ± 63	177 ± 11
J1640+2224	1.2	0.2 ± 0.1	20 ± 4	38 ± 8	75 ± 14
J1713+0747	1.1	0.6 ± 0.2	14 ± 5	82 ± 16	52 ± 2

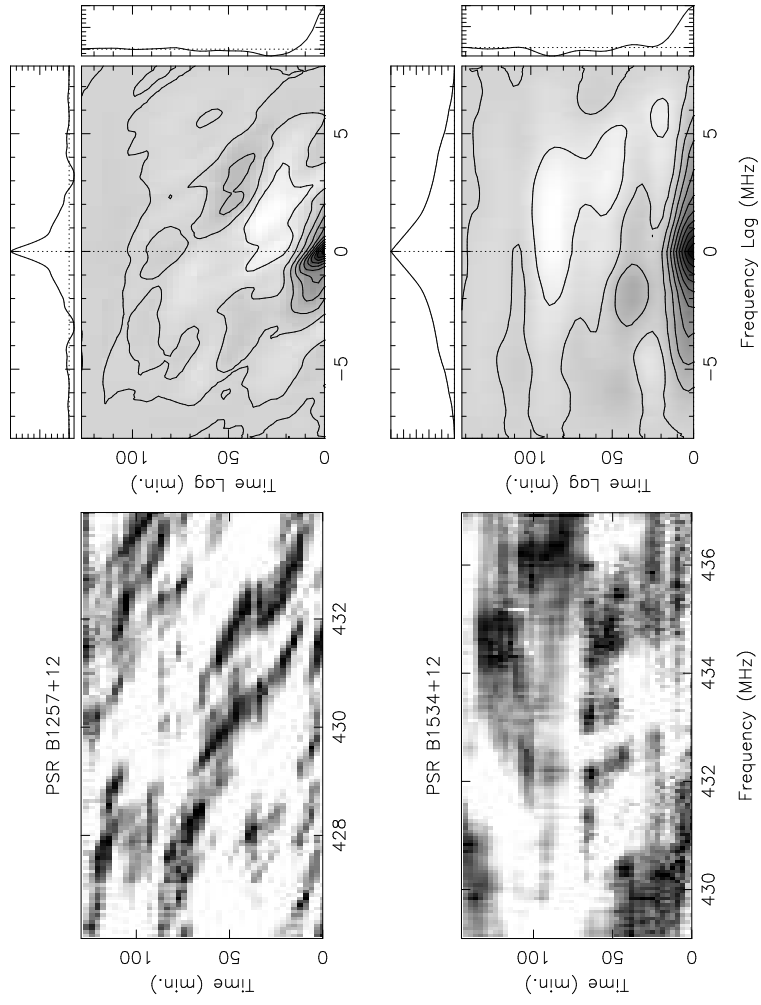


Fig. 1.—

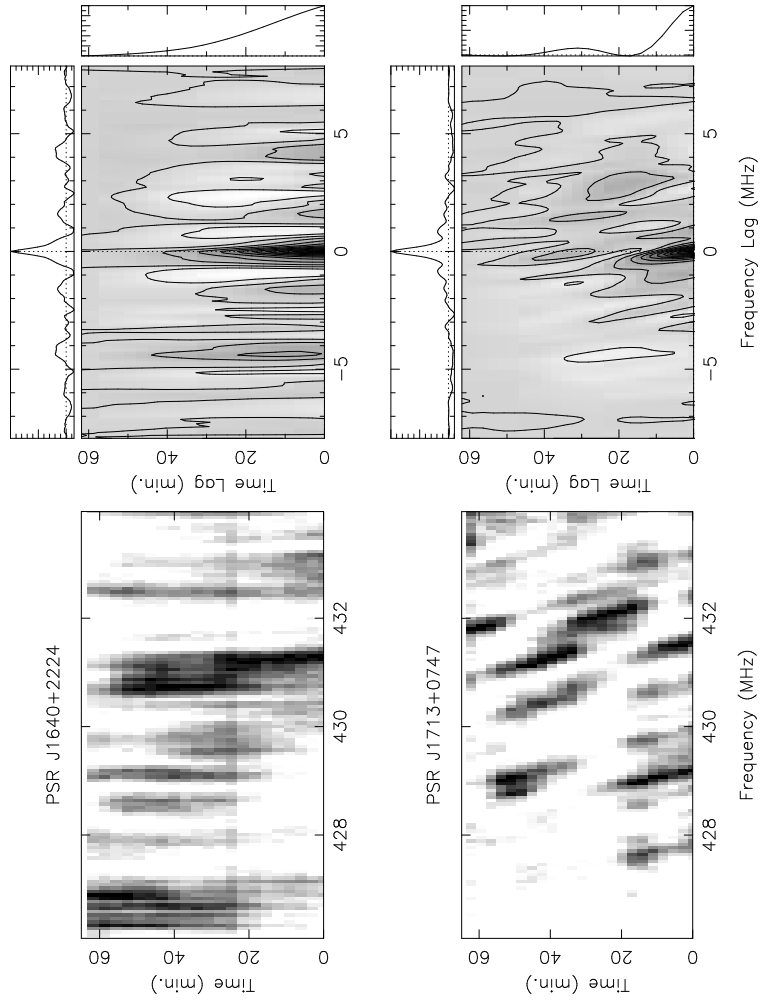


Fig. 2.—

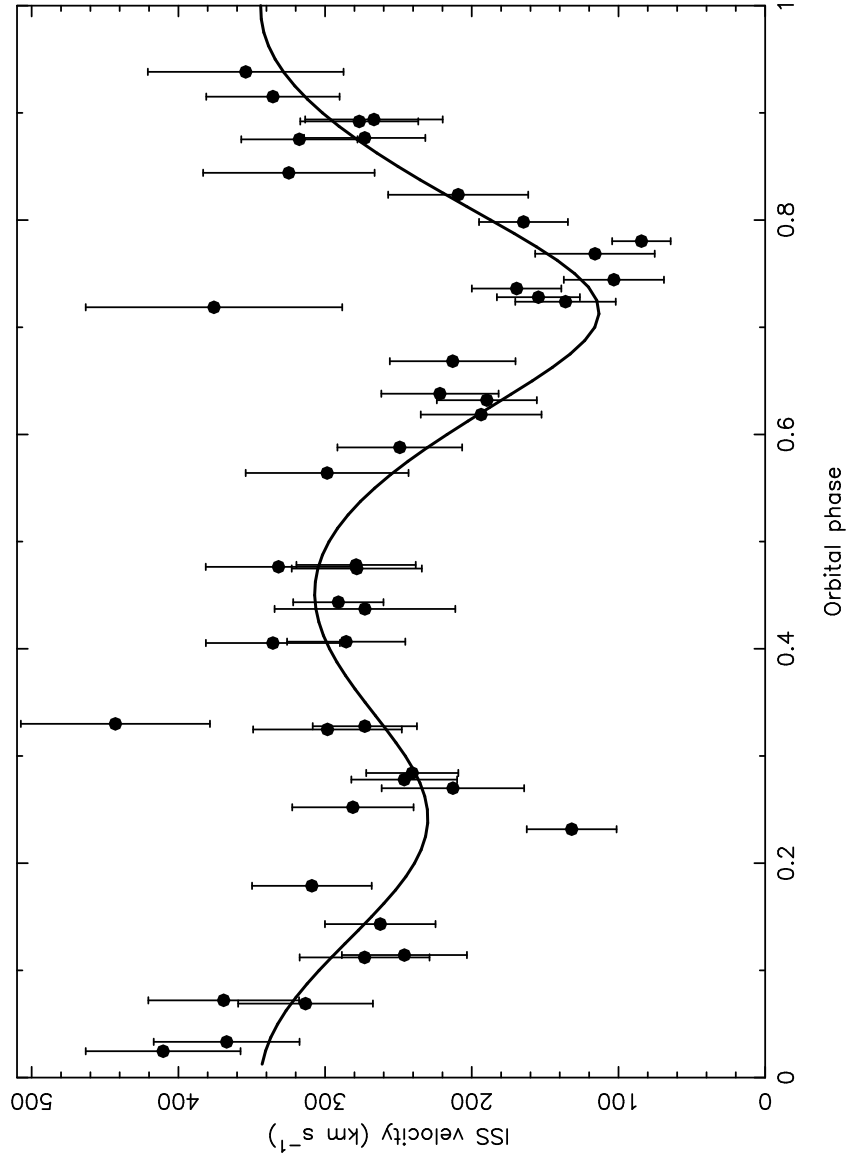


Fig. 3.—